Flow Simulation Through Arteriovenous Fistulae

Jayme Pinto Ortiz
Universidade de São Paulo, Escola Politécnica, Departamento de Engenharia Mecânica – Av. Prof. Mello Moraes, 2231 – Butantã – São Paulo
jportiz@usp.br

Kleiber Lima de Bessa
Universidade de São Paulo, Escola Politécnica, Departamento de Engenharia Mecânica – Av. Prof. Mello Moraes, 2231 – Butantã – São Paulo
kleiber.bessa@poli.usp.br

Abstract. The arteriovenous fistulae (FAV) is a technical surgery which permit the connection between an artery and a vein, so that a fast circulation of artery blood for the vein is allowed. The failures in arteriovenous fistulae, or either, its clogging, are related with the progression of the myointimal hiperplasia. The aetiology of this process is still not known, but the configuration of fistulae and the local haemodynamics have influence in this process. This work has the objective to simulate the flow by comparing some surgical techniques of fistulae: end-to-side and side-to-side. The physiological data had been supplied by Master Program developed at the Experimental Surgery Section of Escola Paulista de Medicina/UNIFESP and the simulations were done using Fluent 5.5 code. The arteries were considered as rigid tubes, the flow was considered steady and 15, 30, 45, 60 and 75 degrees of anastomosis angles were simulated.

Keywords. Hemodynamic; shear stress; fistulae.

1. Introduction

The arteriovenous fistulae (FAV) is a technical surgery which permit the connection between an artery and a vein, so that a fast circulation of artery blood for the vein is allowed. Owens & Bower (1980) reported that this fast circulation of blood occurs because FAV acts as a short circuit between the arterial and venous system, which means that blood flows through the path of lesser resistance. The aperture of fistulae reduces the peripheral resistance and dramatically amplifies the flow through the proximal artery. Sivanesan et al (1999 a) reported that with the increase of the flow through fistulae, a dilatation of the vessel occurs, as an adaptation mechanism, not allowing an extreme increase of the shear stress. In mature fistulae, the proximal vein is enlarged and wall thickness is reduced facilitating the vascular access for hemodialysis.

Although the blood flow is increased after FAV surgery, which is demanded by hemodialysis patients, this kind of surgery causes implications in the walls of the endothelium, which could cause complications in the blood flow. This is known in medical literature as endothelial dysfunction. Caramori & Zago (2000) define the endothelial dysfunction as a disequilibrium between the relaxants factors and constrictors, procoagulants and anticoagulant mediators, or between stimulating and inhibiting substances of the growth and cellular proliferation.

Bakker & Gans (2000) reported that stenosis and, possibly, thrombosis occurs with the development of the intimal hyperplasia in a fibroproliferative as a reply to the endothelial dysfunction. The local development of these stenosis injuries is related with the geometry of fistulae and the hemodynamic of the process. Sivanesan et al (1999 b) comment that both, high and low shear stress, have influence in the permeability of the endothelium for the constituent of the plasma and platelet-derived factors. Low shear stress allows the accumulation of platelet and mitosis and high shear stress can cause damages to the blood cells and endothelial injury.

Honda et al (2001) reported that the atherosclerosis occurs in a non-random distribution within the arterial tree. Asakura & Karino (1990), Ku et al (1985) and Ravensbergen et al (1998) comment that specific regions to occur atherosclerosis are in the arterial bifurcations inside of the coronary, carotid and basilar arteries. Traub & Berk (1998), Zarins et al (1983) and Gibson et al (1993) reported that these regions are characterized by low shear stress and flow reversal. Taylor et al (2002) reported that, in contrast with the effect of low shear stress, higher values of the shear stress induce a cellular structural direct change including the elongation in the direction of the maximum stress and resulting in the inhibition of the arteriosclerosis.

The shear stress has an important paper in the analysis of the arterial flow, therefore studies have identified that this is important for the normal functioning of the cells endothelial. Malek et al (1999) comment that arterial-level shear stress (>1,5 Pa) induces endothelial quiescence and an atheroprotective gene expression profile, while low shear stress (<0,4 Pa), which is prevalent at atherosclerosis-prone sites, stimulates an atherogenic phenotype.

Considering what is said above it is very important to know the hemodynamic factors, which affect the blood flow. This work has the objective to simulate the flow by comparing some surgical techniques of fistulae: end-lateral and side-to-side. The physiological data had been supplied by a Master Program developed at the Experimental Surgery Section of the Escola Paulista de Medicina/UNIFESP described in Galego et al (2000) and the simulations were done using Fluent 5.5 code. As

boundary conditions it was considered the arteries as rigid tube, angles of anastomosis of 15, 30, 45, 60 and 75 degrees, steady flow. The results showed that, in the regions of bifurcations, which is typical on arteriovenous fistulae, recirculation, secondary flows, stagnation points, separation etc, are common, changing the field of shear stress. In these regions are very important a detailed study of the local hemodynamic factors, which is in connection with the objective of the work here presented.

2.Method

2.1.Model Geometry

Two surgical techniques had been considered for computational analysis: end-to-side and side-to-side. The geometric form of the technique end-to-side is "Y" and of the side-to-side is sufficiently similar to "Y". The side-to-side geometry presents as side portion in connection with the vein. This side portion serves as an entrance for surgery cleaning procedure in this region. The Figure (1) below represents the geometry of the two used surgical techniques.
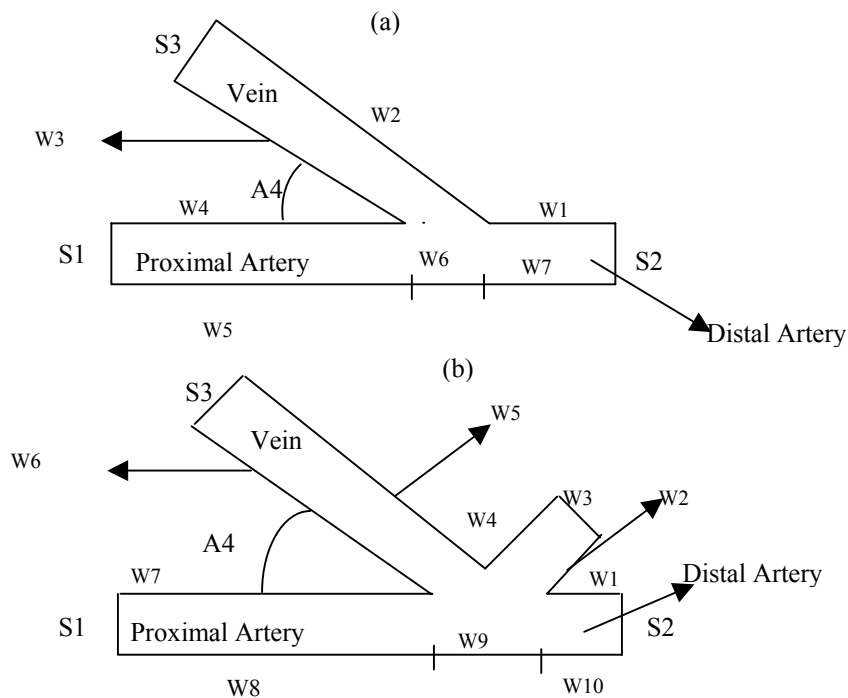
Figure 1. (a) end-to-side: S1 and S2 – inlet section; S3 – outlet section; A4 – angle of anastomosis. (b) side-to-side: S1 and S2 – inlet section; S3 – outlet section; A4 – angle of anastomosis. W(Walls) 2,3,5, 6 and 9 indicate sites at which results are plotted.

The diameter of the artery and vein had been respectively: 4 and 6 mm. The angles of anastomosis had varied from 15 degrees to 75 degrees with increments of 15 degrees. The diameter of the anastomosis is 6 mm. The discretization model was generated by the Gambit software tool. Initially the vertices and, after that, its contours had been defined and finally the faces. After the procedure of creation of the faces the discretization of the domain was carried through. The formation of the mesh is carried through by the specification of nodes in the wall of the artery and the vein. Quadrilaterals elements in the region of the artery and triangular elements in the region of the vein had been generated. Soon after the procedure of generation of the mesh, it had been defined, in the Gambit, the regions of entrance and exit of control volume flow: velocity inlet (S1 and S2) and pressure outlet (S3). The remaining regions had been called "walls" and to each one, a numerical number was attributed. The computational domain for the two surgical techniques is represented in Fig. (2). After the ending of mesh generation this was exported from Gambit to the Fluent code.
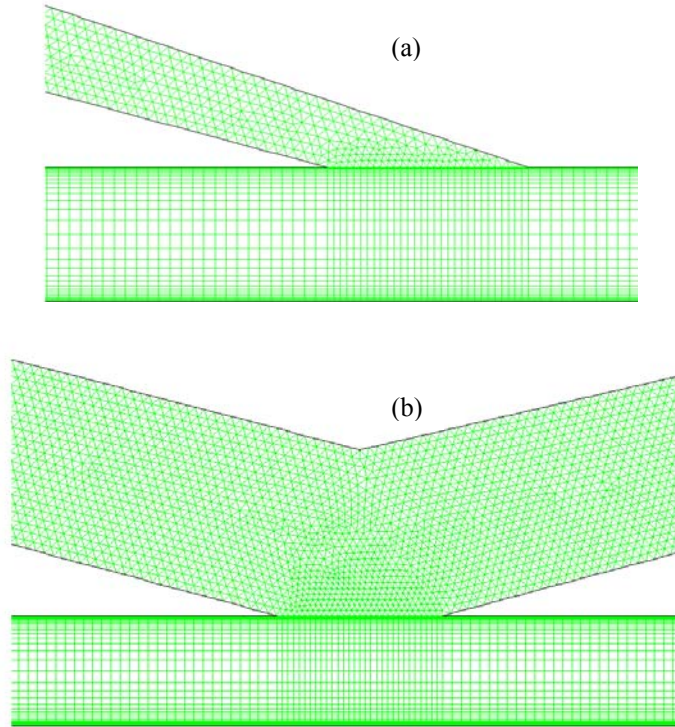
Figure 2. Grid computational: (a) end-to-side; (b) side-to-side. (No scale in figure).

2.2.Numerical model and flow conditions

The absolute viscosity of the blood is $4*10^{-3}$ kg/ms. Blood flow through the fistulae has the attributes of bi-dimensional, steady, incompressible, isothermal flow. The mathematical equations governing the flow are:

$$\nabla.\vec{u} = 0 \quad \text{continuity equation,} \tag{1}$$

$$\left(\vec{u}.\nabla\right)\vec{u} = -\frac{\nabla p}{\rho} + \nu\nabla^2\vec{u} \qquad \text{Navier-Stokes equation,} \tag{2}$$

where $\boldsymbol{u}$ is the velocity vector, ρ is the density, p is the pressure, and ν cinematic viscosity. The CFD flow solver, FLUENT Inc. (v 5.5) (academic version), was employed to obtain a numerical solution to the governing equations. The discretization of the equations for each control volume was obtained using the first order upwind scheme. The set of the algebraic equations had been solved iteratively using the procedure based on the semi-implicit SIMPLE algorithm.

The simulations had been carried through under physiological conditions (Galego 1998) carried through some flow measurements in the proximal artery (Q1) and distal artery (Q2) using the electromagnetic flow meter. These data had been used in this work, which correspond to values of Q1 = 300 ml/min e Q2 = 120 ml/min, resulting in the vein (Q3) a value of 420 ml/min. The Reynolds number in the vein is of the order of 430.

The no-slip conditions was applied at all walls.

3.Results

3.1.Flow behavior

Through the comparison of the velocity fields for the two fistulae, we perceive that it has similarities in the behaviors of these velocity fields. The zones of separation and recirculation are similar for the two techniques. The points of stagnation of the fluid are similar. However, when we occluded distal artery, it was founding new point of stagnation and zones of recirculation.

Both FAV end-to-side and side-to-side present an adverse pressure gradient in W6 and W9, respectively (fig.3). This can be seen by the inversion in the direction of the velocity fields.
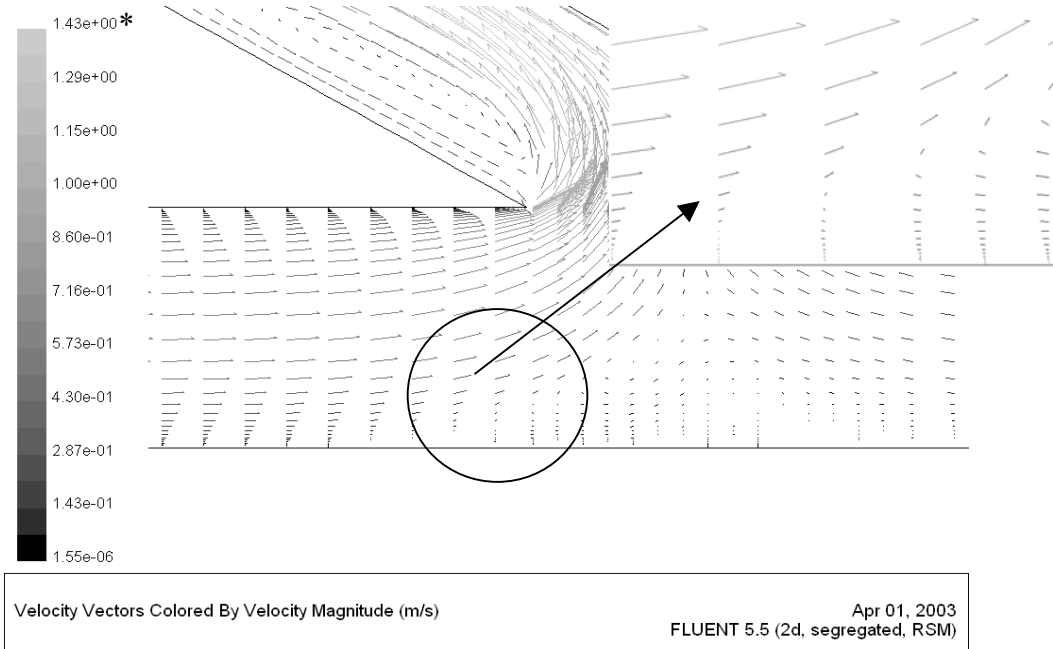
Figure 3. Velocity vectors in the fistulae end-to-side (30º). *Outflow equal 420 ml/min.

Zones of recirculation and stagnant fluid occurs in walls 6 and 9 of fistulae end-to-side and side-to-side, respectively (fig. 4a and 4b). This zone of recirculation does not occupy all the transversal section of the artery. However, when we have flow only through the proximal artery, this zone of recirculation occupies all the region of the anastomosis (fig.4c and 4d).
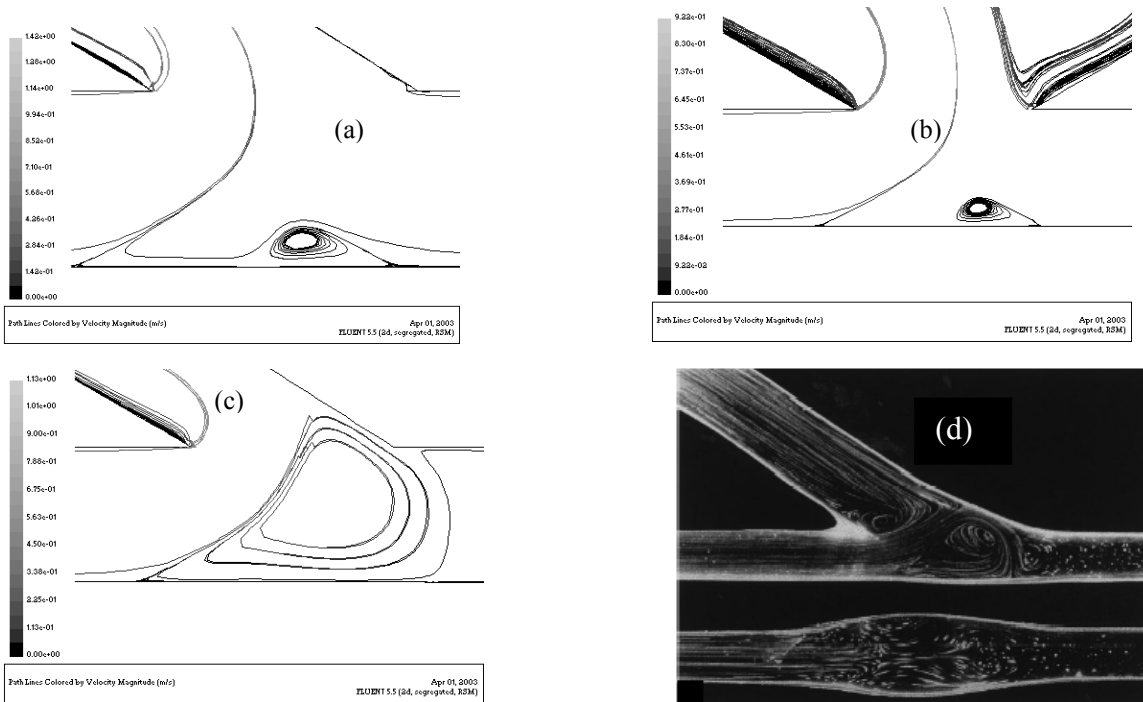
Figure 4. Path lines by velocity magnitude (m/s). All the graphs had been represented for outflow of 420 ml/min.

Sivanesan et al (1999 b) using photographic techniques visualized the draining in FAV end-to-side, considering the flow only in the proximal artery. The Figure 4c and 4d above represents the flow only in the proximal artery. As the fluid of the proximal artery enters in the anastomosis, a separation and a vortex in the anticlockwise rotation is formed. Wall 2 and wall5 of FAV end-to-side and side-to-side respectively suffers impact from the fluid which is coming from the proximal artery. After the impact, the fluid separates, forming a vortex in the clock-wise rotation that occupies great part of the anastomosis.

Sivanesan et al (1999 c) presented some types of stenosis in FAV and classified these as stenosis type 1,2 and 3. Stenosis of type 1 is situated respectively in wall 6 and 9 of the FAV end-to-side and side-to-side. One of the proposals theories for the development of stenosis in these places would be the low shear stress in the wall which would take the accumulation of platelet and mitosis. Stenosis of type 2 appears respectively in walls 3 and 6 of the FAV end-to-side and side-to-side, respectively. In the region of stenosis type 2, the value of the shear stress is greater than the values for development of the atherosclerosis (see Fig. 9). In this region, there is a point of stagnation of the fluid (see Fig. 5a and 5b). The point of stagnation of the fluid can be a preponderant factor for the appearance of stenosis type 2.
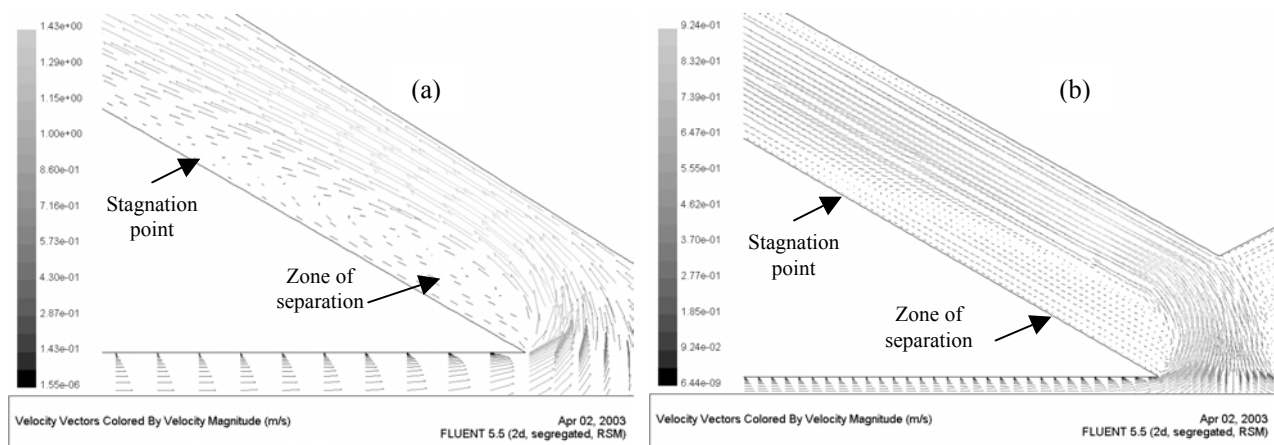
Figure 5. Velocity vectors by velocity magnitude presenting stagnation point and zone of separation. The graphs are with Outflow of Q3 = 420 ml/min

The length of the separation region of the draining grows in wall 3 with the increase of the angle of anastomosis in the FAV end-to-side; the same happens for the FAV side-to-side until 45 degrees. In the range of 45 to 60 degrees this length does not grow and, in the range 60 to 75 degrees this length diminishes in FAV side-to-side. These values can be observed by Tab (1) and Fig. (6).

Table 1. Values of separation the lengths zone in walls 3 and 6 of the FAV end-to-side and side-to-side. Angles of anastomosis in between 15 to 75 degrees.

	FAV end-to-side	FAV side-to-side
Angle of Anastomosis	L (mm)	L (mm)
15	1,5	5
30	3	9
45	8,5	12
60	11	12
75	14	6

The analysis of results of Tab.(1) shows that the length of the separation zone is higher in the FAV side-to-side and increases until the angle of 60 degrees. For the angle of 75 degrees the geometry of the FAV side-to-side force the fluid to shock more quickly with wall 6, which is the probable reason for the length of the separation zone diminishes.
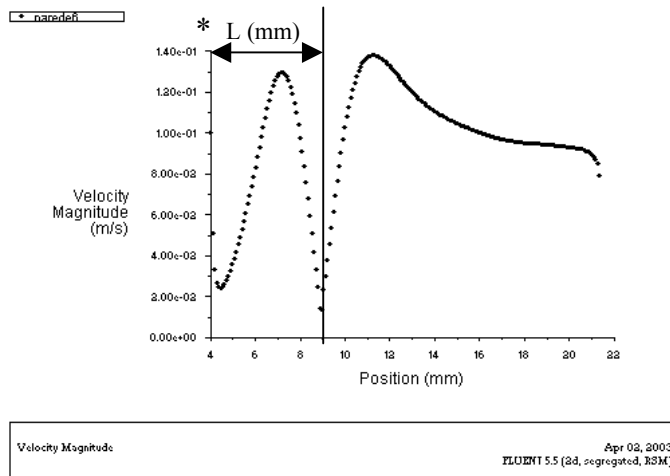
Figure 6. Length of separation zone (L). * Q3 = 420 ml/min.

3.2. Wall Shear Stress Distribution

Figure 7 below, shows the results of shear stress distribution in wall 2 of the FAV end-to-side for the angles (15, 45, and 75 degrees). It is clear in Fig. 7 that with the increase of the anastomosis angle the behavior of the distribution of the stress is similar, however the peak of the shear stress is reduced. The values of the shear stress of the FAV end-to-side for all the angles are shown in Tab. (2).
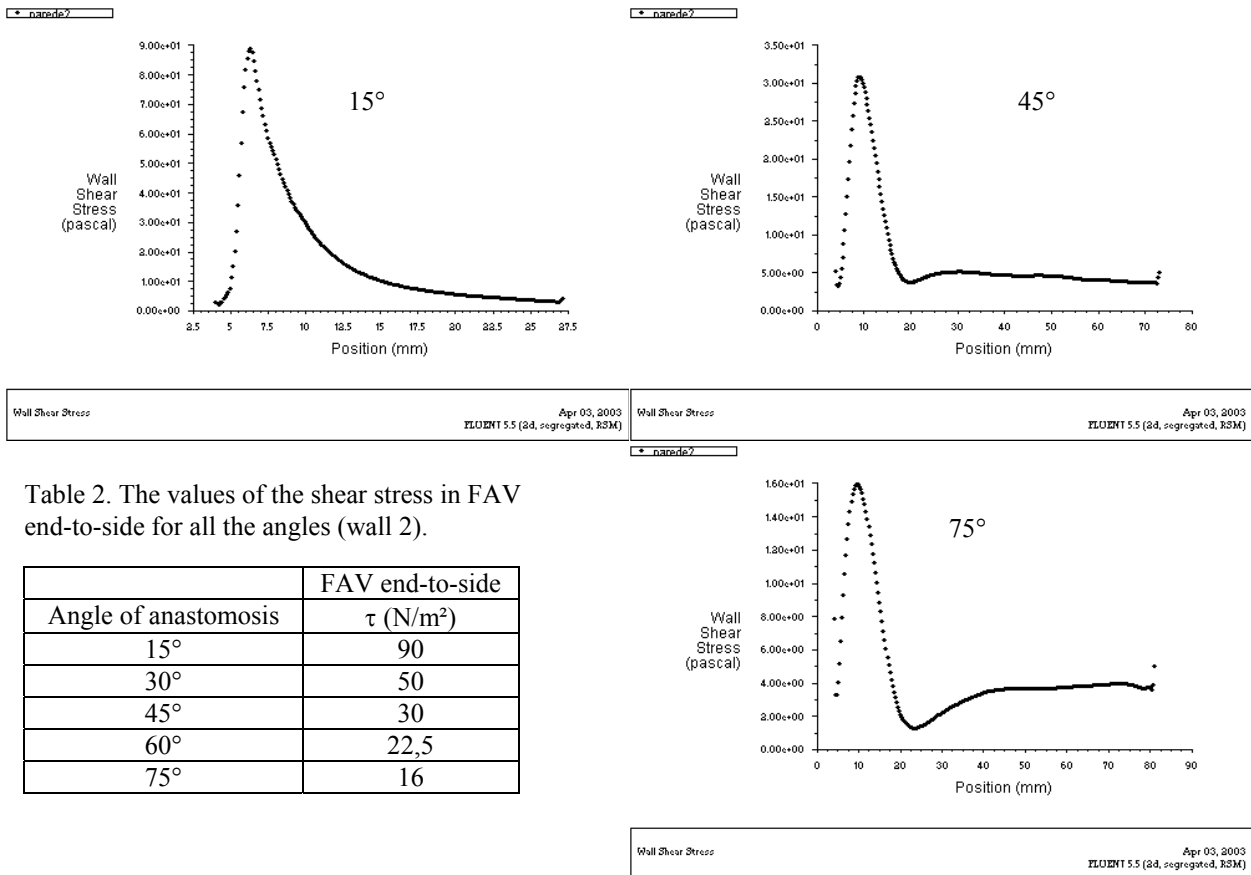
Table 2. The values of the shear stress in FAV end-to-side for all the angles (wall 2).

	FAV end-to-side
Angle of anastomosis	τ (N/m²)
15°	90
30°	50
45°	30
60°	22,5
75°	16

Figure 7. Distribution of the shear stress in the FAV end-to-side with the variation of the anastomosis angle. Q3 = 420 ml/min.

The distribution of the shear stress in wall 5 for the FAV side-to-side is represented in the Fig. (8) with variation in the anastomosis angles. As in the case of the FAV end-to-side, in the FAV side-to-side the peak of the shear stress also diminishes with the increase of the anastomosis angles, however with less significant reductions. The values of the shear stress of the FAV end-to-side for all the angles are shown in Tab. (3).
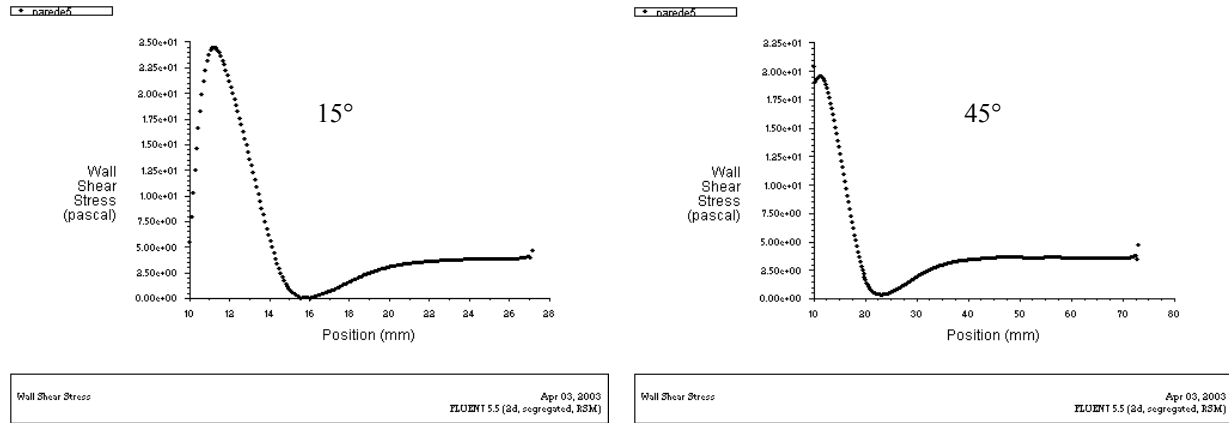
Table 3. The values of the shear stress in FAV end-to-side for all the angles (wall 5).

	FAV side-to-side
Angle of anastomosis	τ (N/m²)
15°	25
30°	22,5
45°	20
60°	15
75°	10
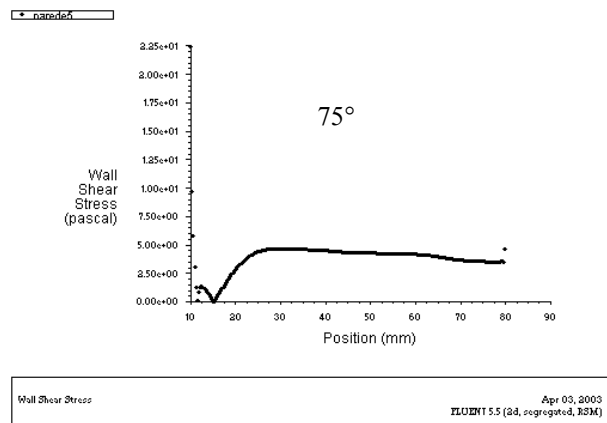
Figure 8. Distribution of the shear stress in the FAV end-to-side with the variation of the anastomosis angle. Q3 = 420 ml/min.

The shear stress in wall 6 and 9 of the FAV end-to-side and side-to-side respectively, presented lower values of magnitudes compared with the values in walls 2 and 5 of these FAV. The values of this stress are shown in the Tab. (4) below for the FAV end-to-side and side-to-side with the variation of the anastomosis angles. Sivanesan (1999 b) classified this region as stenosis type 1.

Table 4. Shear stress in wall 6 and 9 of the FAV end-to-side and side-to-side, respectively (Q3 = 420ml/min).

	FAV end-to-side	FAV side-to-side
Angle of anastomosis	τ (N/m²)	τ (N/m²)
15°	0,36	0,51
30°	0,41	0,51
45°	0,47	0,52
60°	0,5	0,53
75°	0,53	0,52

4.Discussion

The shear stress is one of the primordial factors for the hemodynamic analysis in FAV. Fung (1997) shows some regions of values of shear stress relating it with biological effect (Fig. 9). The results of shear stress obtained in this work are on Fig. (9).

By analysis of the range of values of shear stress of Fung (1997) corresponding with atherosclerosis occurrence and comparing this values with our results (W6 and W9, respectively end-to-side and side-to-side), we perceive that our values of tension are inside of this range. For the FAV end-to-side, the values of shear stress in W6 are modified with the increasing of the angle of anastomosis (see Tab.(4)), however inside the range of corresponding stress atherosclerosis. For the FAV side-to-side, the values of shear stress (W9) are practically constant with the variation of the anastomosis angle and presenting higher values compared with the FAV end-to-side values (see Tab.(4)),but without leaving the range associated to atherosclerosis.

The shear stress in wall 2 of the FAV end-to-side for angles of 15,30 and 45 degrees had presented values greater that 30 Pa (see Tab.(2)). In wall 5 of the FAV side-to-side the values of shear stress are smaller that 30 Pa (see Tab.(3)). Fry (1968) and Malek et al (1999) comment that values of shear stress in the range of 35 to 40 Pa, can cause damages in endothelial cells. The results for FAV side-to-side shows shear stress in a smaller range (10 to 25 Pa), however, the results for FAV end-to-side show shear stress in a higher range. Taking in consideration these results, the FAV end-to-side can cause direct injury to the endothelial cells.
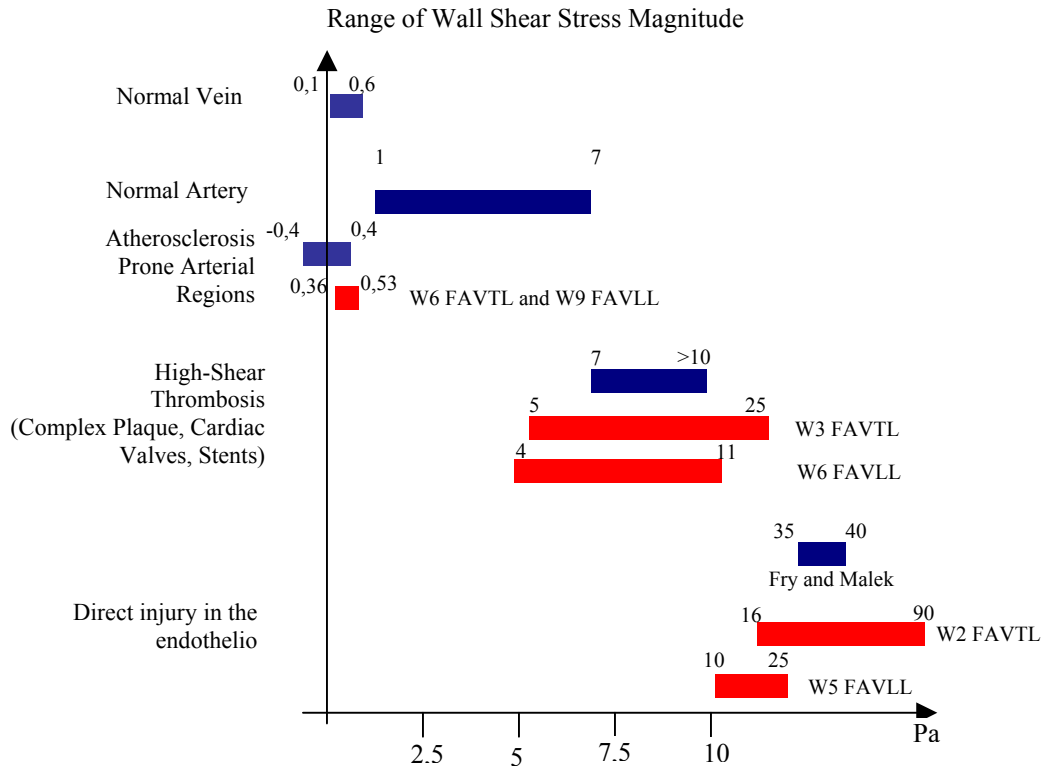
Figure 9. Shear stress band values in artery and vein walls. Data from literature in blue. Data from this work in red.

In wall 3 of the FAV end-to-side, with the increase of the anastomosis angle the shear stress varies in the range of 5 to 25 Pa. For wall 6 of the FAV side-to-side, also, with the increase of the anastomosis angle, the shear stress varies in the range of 4 to 11 Pa. According with the literature (7 to 10 Pa), in this range of shear stress the occurrence of thrombosis is possible.

The shear stress values in wall 6 and wall 9 of FAV end-to-side and FAV side-to-side respectively (0,36 to 0,53 Pa), are nearly in the range values of literature (-0,4 to 0,4 Pa) that can cause atherosclerosis.

It is possible to conclude from this work that it is important to know the velocity field in FAV to improve the different surgical techniques.

5. Acknowledgement

6. References

Asakura, T., Karino, T., 1990, "Flow patterns and spatial distribution of atherosclerotic lesions in human coronary arteries", Circulation Res, Vol 66, pp. 1045-1066.

Bakker, S.J.L., Gans, R.O.B., 2000, "About the role of shear stress in atherogenesis", Cardiovascular Research, Vol. 45, pp. 270-272.

Caramori, P.R.A., Zago, A.J., 2000, "Disfunção Endotelial e Doença Arterial Coronariana", Arq Bras Cardiol, Vol. 75, pp. 165-172.

Fry, D.L., 1968, "Acute vascular endothelial changes associated with increased blood velocity gradients", Circulation Research, Vol. 22, pp. 165-197.

Fung, Y.,C., 1997, "Biomechanics: Circulation", Springer, New York, New York, 571 p.

Galego, S.J., 1998, "Estudo comparativo do fluxo nas fístulas arteriovenosas femorais, término-lateral e látero-lateral modificada em cães". Dissertação de Mestrado, Escola Paulista de Medicina/UNIFESP, 80 p.

Galego, S.J., Goldenberg, S., Ortiz, J.P., Gomes, P.O., and Ramacciotti, E., 2000, "Comparative blood flow study of arteriovenous fistulae in canine femoral arteries: modified latero-lateral and end-lateral techniques", Artificial Organs, Vol. 24, pp. 235-240.

Gibson, C.M., Diaz, L., Kandarpa, K., 1993, "Relation of vessel wall shear stress to atherosclerosis progression in human coronary arteries", Arterioscler Thromb, Vol. 13, pp. 310-315.

Honda, H.M., Hsiai, T., Wortham, C.M., Chen, M., Lin, H., Navab, M., Demer, L.L., 2001, "A complex flow pattern of low shear stress and flow reversal promotes monocyte binding to endothelial cells", Atherosclerosis, Vol 158, pp. 385-390.

Ku, D.N., Giddens, D.P., Zarins, C.K., Glagov, S., 1985, "Pulsatile flow and atherosclerosis in the human carotid bifurcation. Positive correlation between plaque location and low oscillating shear stress", Arteriosclerosis, Vol. 5, pp. 293-302.

Malek, A.M., Alper, S.L., Izumo, S., 1999, "Hemodynamic Shear Stress and Its Role in Atheroscerosis". JAMA, Vol 282, pp. 2035-2042.

Owens, M.L., Bower, R.W., 1980, "Physiology of arteriovenous fistulas", In: Wilson SE, Owens ML, eds. Vascular Access Surgery. Year Book Medical Publishers, Chicago, pp. 101-114.

Ravensbergen, J., Ravensbergen, J.W., Krijger, J.K., Hillen, B., Hoogstraten, H.W., 1998, "Localizing role of hemodynamics in atherosclerosis in several human vertebrobasilar junction geometries", Arteriosc Thromb Vasc Biol, Vol. 18, pp. 708-716.

Sivanesan, S., How, T.V., Bakran, A., 1999 a, "Characterizing flow distributions in AV fistulae for haemodialysis access", Nephrology Dialysis Transplantation, Vol. 13, pp. 3108-3110.

Sivanesan, S., How, T.V., Bakran, A., 1999 b, "Flow patterns in the radiocephalic arteriovenous fistula: an in vitro study", Journal of Biomechanics, Vol. 32, pp. 915-925.

Sivanesan, S., How, T.V., Bakran, A., 1999 c, "Sites of stenosis in AV fistulae for haemodialysis access", Nephrol Dial Transplant, Vol. 14, pp. 118-120.

Taylor, C.A., Cheng, C.P., Espinosa, L.A., Tang, B.T., Pakker, D., Herfkens, R.,J., 2002, "In vivo quantification of blood flow and wall shear stress in the human abdominal aorta during lower limb exercise", Annals of Biomedical Engineering, Vol. 30, pp. 402 – 408.

Traub, O., Berk, B.C., 1998, "Laminar Shear Stress – Mechanisms by which endothelial cells transduce an atheroprotective force", Arterioscler Thromb Vasc Biol., Vol 18, pp. 667-685.

Zarins, C.K., Giddens, D.P., Bharadvaj, B.K., Sottiurai, V.S., Mabon, R.F., Glagov, S., 1983, "Carotid bifurcation atherosclerosis: Quantitative correlation of plaque localization with flow velocity profiles and wall shear stress", Circ. Res., Vol 53, pp. 502-514.

7. Copyright Notice